

Energy Selective Surface Superstrate on Antenna both Gain Enhancement and HPM Protection

Adem Kocyigit^{1,2}^a, Burak Çelik³^b, Mahmut Burak Karadeniz³^c, Onur Arsali³^d, Ebru Efeoğlu⁴^e and Bahattin Turetken³^f

¹*Institute of Science, Electronics and Telecommunication Engineering, Kocaeli University, Umuttepe, Kocaeli, Turkey*

²*Department of Electronics and Automation, Bilecik Seyh Edebali University, Gulumbe, Bilecik, Turkey*

³*Department of Electronics and Telecommunication Engineering, Kocaeli University, Umuttepe, Kocaeli, Turkey*

⁴*Department of Software Engineering, Kütahya Dumlupınar University, Kütahya, Turkey*

Keywords: Energy Selective Surfaces, ESS, Superstrate, HPM Protection.

Abstract: Energy selective surfaces (ESS) have gained great interest for one decade to protect vulnerable electronic devices due to their adaptive surfaces against the power of electromagnetic waves. In this study, we designed a double layer ESS structure both to enhance gain of an antenna in the case of low power electromagnetic waves and to protect it against high-power microwave (HPM) or electromagnetic pulse (EMP). The antenna was designed by using Rogers RT5880 substrate as rectangular patch with a line feed for the 2.45 ISM (Industrial, Scientific, and Medical) band. The ESS layers as arrays were placed on the antenna as superstrate by a distance. The design results revealed that ESS superstrate layers can increase gain of antenna in the transmission band and protect antenna in the case of HPM. The ESS layers can be act as both superstrate and protection layers at the same time.

1 INTRODUCTION

Antennas need to be protected against HPM and EMP because they are the opening door to the outside of the electronic parts of vehicles such as aircraft and unmanned aerial vehicles (Huang et al., 2022). These are realized with materials such as active absorber metasurfaces (Luo et al., 2023), frequency selective surfaces (FSS) (Chatterjee et al., 2024), plasma confinements (L. Wang et al., 2022), ceramic-based film materials (Zurauskiene et al., 2013) and large magnetoresistive materials (Pannetier-Lecoeur et al., 2007). The ESS is a field-induced surface sensitive to the field intensity of the incident wave, is first proposed by Liu et al. in a patent in 2009, and it has been published as a paper in 2013 (Yang et al., 2013). ESS structures which are typically designed as a two-dimensional array, are integrated into the front end of

a radar system or as a protective layer on an antenna, operating as a power-dependent switch in free space (Qin & Zhang, 2019). These structures have been quite popular since 2017 and have attracted the attention of many scientists (Gong & Zhang, 2021; Hu et al., 2024; Zhang et al., 2019).

Metamaterials (MTM), FSS or partially selective surface (PRS) periodic structures are used as antenna superstrate layers to enhance the performance of planar antennas (K & Pradeep, 2022; Kangeyan & Karthikeyan, 2024). The efficiency, bandwidth, and gain of planar patch antennas can be successfully increased with antenna superstrates, and that these antennas can be easily used in a wide variety of applications, such as health monitoring and communications (K.Sumathi et al., 2021; Melouki et al., 2022). Sumathi et al. (2021) showed that the operating frequency of the antenna can be configured by using MTM multilayered superstrates and adding

^a <https://orcid.org/0000-0002-8502-2860>

^b <https://orcid.org/0000-0002-3204-5444>

^c <https://orcid.org/0000-0002-6645-2734>

^d <https://orcid.org/0009-0005-0170-3968>

^e <https://orcid.org/0000-0001-5444-6647>

^f <https://orcid.org/0000-0001-5451-7089>

diodes to them, and the gain can be increased from 3.66 dB to 7.36 dB by configuring the diodes (K.Sumathi et al., 2021). In a study carried out by Dey and Dey (2023), a broad-band miniaturized Fabry-Perot cavity resonator antenna fabricated of a new electromagnetic band gap (EBG) superstrate as a rectangular patch antenna supported by PRS and reactive impedance surface (RIS) was used, with a bandwidth between 9.91 and 12.71 GHz (24.8) and a gain increase of 6.59 dB compared to the reference antenna was achieved (Dey & Dey, 2023). Abdelaziz et al. (2023) designed a multiple-input multiple-output (MIMO) circular spiral patch antenna using a bifacial logarithmic spiral metamaterial superstrate which acts as new planar concave-concave lens for circularly polarized (CP) antenna system which are used in 5G applications and the proposed top layer increased the isolation, gain and bandwidth of the antenna by about 32 dB, 3.47 dB and 900 MHz respectively (Abdelaziz et al., 2023). Nguyen and Seo (2023) demonstrated 33% bandwidth, -14.3 dBi maximum peak gain, and a low specific absorption ratio (SAR) by integrating a drilled ground plane (DGS) and a holed dielectric superstrate layer operating at a center frequency of 2.4 GHz to achieve CP characteristics of an ultraminiature antenna and gain enhancement (Nguyen & Seo, 2023).

According to our best knowledge, there are no studies in the literature that use ESS structure as the antenna top layer which both to protect the antenna from high power electromagnetic waves and to improve its performance. This study aims to improve antenna performance while protecting antenna from HPM or EMP by using ESS surfaces as the superstrate. In this study, we have designed a patch antenna for 2.45 GHz ISM band and superstrate ESS layer to improve antenna properties at transmission band and to protect antenna from HPM when the diodes are in the ON state.

2 DESIGN OF ANTENNA AND ESS STRUCTURES

In the modelling of ESS structures, a standard FSS or metamaterial structure is constructed, and the patch elements of these structures are connected to each other by lumped diode elements exhibiting nonlinear properties. Figure 1A shows the equivalent capacitance and inductance model of a structure designed as an ESS in an electromagnetic wave environment. As can be seen here, the gaps between the metal conductors exhibit capacitance properties, while the metal conductors exhibit inductance properties. Figure 1B shows the equivalent circuit model of the PIN diodes used in ESS structures and

simplified representations of them in the OFF and ON states. Here, the diodes are represented by a capacitance when OFF state, and when the diodes are triggered or ON state by the HPM, they are represented by an inductance and a low resistance connected in series (K. Wang et al., 2017).

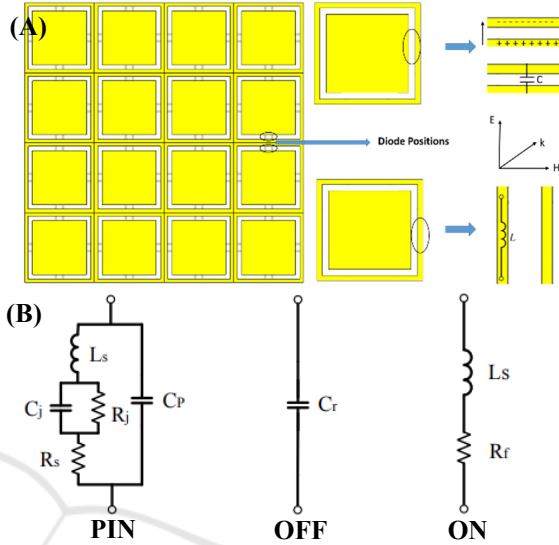


Figure 1: A) Representation of the structures of the ESS surface in the electromagnetic wave environment with equivalent capacitance and inductance. B) Equivalent circuit model of a PIN diode, simplified circuit representation in the OFF and ON states, from left to right, respectively (K. Wang et al., 2017).

The model of antenna and ESS were designed by using CST Microwave Studio. Antenna was designed on the Rogers RT5880 with the thickness of 1.52 mm. Top view of antenna and other related design specifications are displayed in Figure 2.

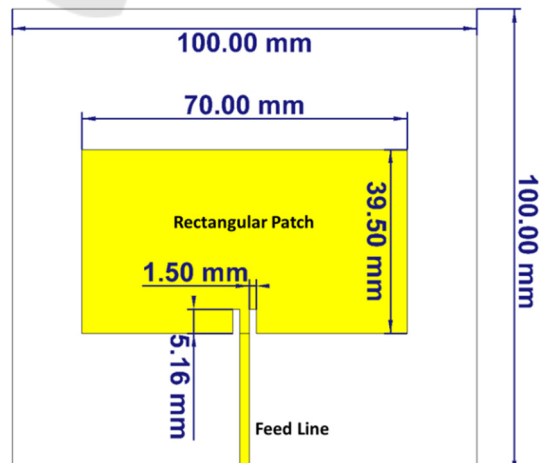


Figure 2: Top view of the antenna and its dimensions.

The ESS structure has been designed on the FR-4 substrates with 1.6 mm thicknesses as double layers. While Figure 3A display ESS unit cell for 3D and side views, Figure 3B indicates front-back and middle layers. The dimension of the substrate was determined as 12 mm. The cross length and width on the front surface were 6.5 mm and 3.5 mm. The radius of side circles was 6.5 mm. The distance between the layers, which are diode placed, is 0.8 mm. The square ring width in middle is determined 0.5 mm after optimization of all parameters. The unit cell was used to obtain superstrate array with 12×12 on the antenna to test antenna performance in the case of transmission and reflection.

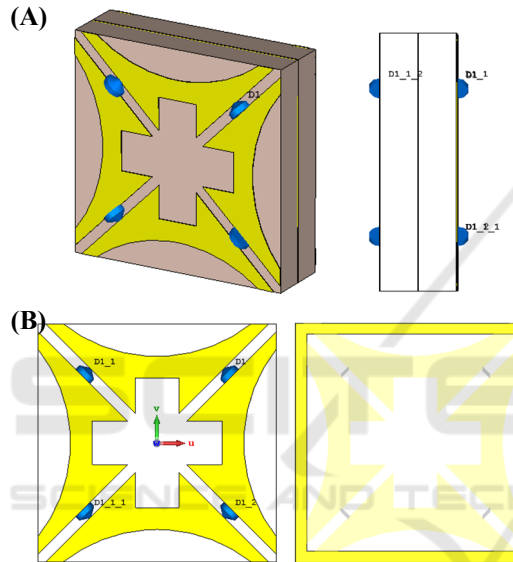


Figure 3: A) 3D (left) and side (right) view and B) front-back and middle layers of the designed ESS unit cell

3 RESULTS AND DISCUSSION

The return loss (S_{11}) graph of antenna has been illustrated in Figure 4. The inset of Fig. 4 exhibits polar radiation pattern of antenna for 2.45 GHz centre frequency. The main lobe magnitude for linear scaling is 6.45 with 5 degrees direction. Side lobe level of the antenna is -20 dB. The efficiency of the antenna was determined to be 88.25%.

The transmission characteristics of ESS unit cell is shown in Figure 5 with return loss and transmission coefficient (S_{21}) in the case of when the diodes are in the OFF and ON states. The equivalent capacitance (C) is determined as 0.2 pF and 0, respectively, in these states. The ESS has two transmission bands in the centre frequency of 2.40 GHz and 4.05 GHz. When the diodes are in the ON state, the ESS provides

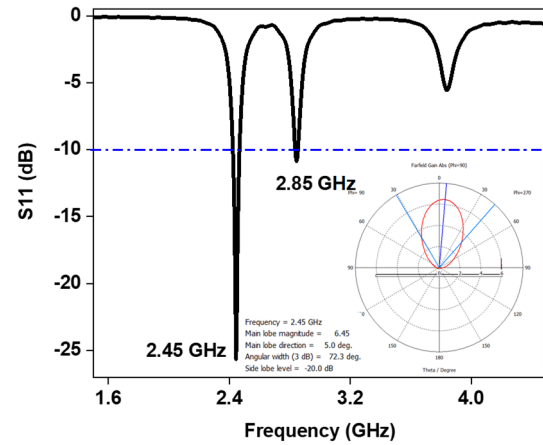


Figure 4: S_{11} graph of the antenna. The inset shows the polar radiation pattern at 2.45 GHz

shielding efficiency less than -25 dB at approximately 2.40 GHz and less than -20 dB for a wide band of 0-4 GHz. The insertion loss for transmission is obtained to be -0.39 dB. The obtained results are good agreement with literature (Zhou et al., 2021).

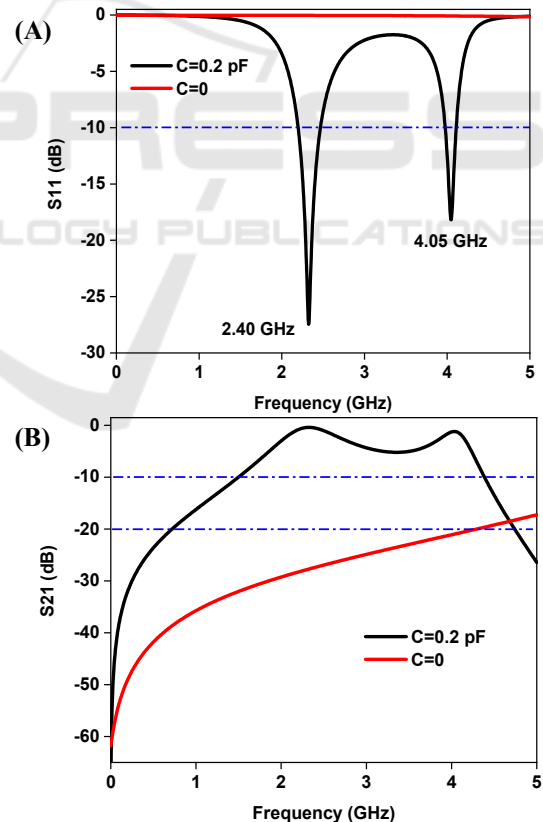


Figure 5: A) S_{11} and B) S_{21} graphs of ESS unit cell for ON/OFF diode states.

The ESS unit cells were transformed the array and used as superstrate layer on the antenna by a distance of 32 mm. Figure 6A shows S_{11} graphs of the reference antenna and antenna-superstrate system. When the diodes are in the OFF state ($C=0.2$ pF), the S_{11} profile almost was not affected from the superstrate layer and the radiation pattern almost did not change much. Main lobe is increased from 6.45 to 6.71. In the case of triggering or in the ON state of the diodes, the transmission is declined. Figure 6B shows peak gain graphs of the reference antenna and antenna-superstrate system. Whereas the gain of reference antenna is obtained as 8.09 dBi, the peak gain increased to 12.24 dBi with ESS superstrate for diodes were in the OFF state. When the diodes are in the ON state in the ESS superstrate, the protection mode has been activated and gain decrease to 2.45 dBi as shown in the broadband gain graphs at 2.45 GHz frequency.

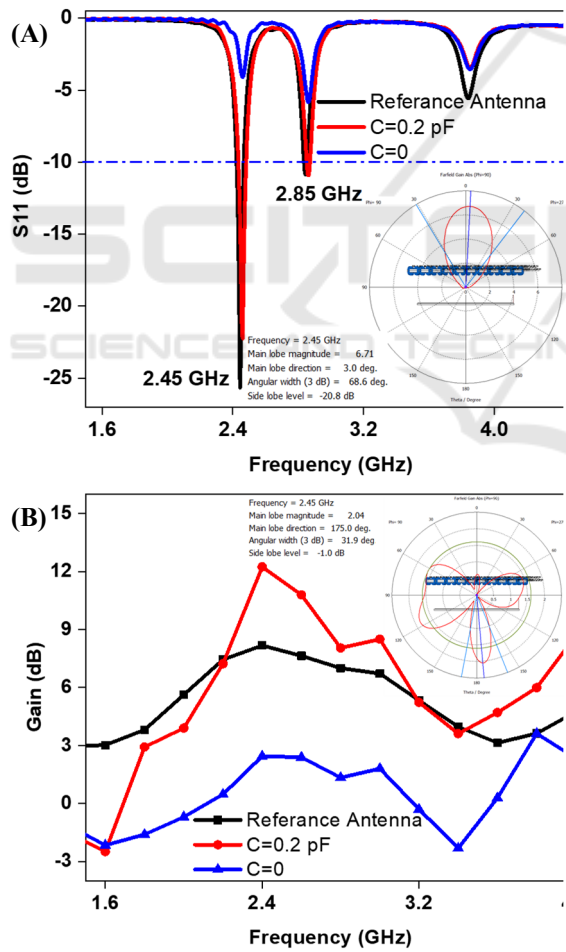


Figure 6: A) S_{11} graphs of antenna with ESS superstrate. B) Broadband gain graphs of reference antenna and antenna-

superstrate system for the case of diodes are in the ON and OFF states.

Table 1 indicates performance of the reference antenna and antenna-superstrate systems for diodes are in the ON state. These values were obtained from 3D Farfield plots of antennas. While the resonance frequency did not change with antenna types, the S_{11} parameters and efficiency of antenna slightly changed for superstrate layer with diodes were in the OFF state. However, the S_{11} parameter increased -4.13 dB and gain decreased to 2.04 dBi with 175 degrees after diodes were in the ON state (Inset of Figure 6B). Furthermore, the bandwidth of the antenna increased from 44.00 MHz to 48.40 MHz by ESS as superstrate layer. These results confirm enhancement of the antenna performance in the transmission states and protection of antenna in case of HPM.

Table 1: Performances of the antennas with and without superstrate for the diodes are in the ON or OFF states

Antenna	S_{11} (dB)	Freq. (GHz)	Efficiency (%)	Gain (dBi)	BW (MHz)
Reference Antenna	-25.61	2.44	88.25	8.09	44.00
Antenna with Superstrate (OFF State)	-22.28	2.46	79.23	8.26	48.40
Antenna with Superstrate (ON State)	-4.13	2.46	30.84	2.04	-

4 CONCLUSIONS

We designed double-layer ESS structures was motivated by two primary goals: enhancing the antenna's gain in the presence of low-power electromagnetic waves and ensuring its protection against HPM or EMP attacks. The design of antenna incorporates a rectangular patch with a line feed using a Rogers RT5880 substrate for the 2.45 ISM band. We placed the ESS layers with arrays above the antenna as a superstrate layer. The results show that ESS superstrate layers (diodes are in the OFF states) can boost antenna gain up to 12.24 dBi in the transmission band without change other antenna parameters and shield antenna against HPM when the diodes are in the ON state. Thus, the proposed ESS structure serves as both a performance-enhancing superstrate and a protective layer against high-power electromagnetic threats.

ACKNOWLEDGEMENTS

Authors would like to thanks Kocaeli University BAP Coordination Unit, project number FDK-2024-3576.

REFERENCES

Abdelaziz, A., Mohamed, H. A., & Hamad, E. K. I. (2023). Performance analysis of double-face logarithmic spiral metasurface superstrate for full enhancement of circularly polarized 5G spiral patch antenna investigated using characteristic mode analysis. *International Journal of Microwave and Wireless Technologies*, 15(1), 129–142. <https://doi.org/10.1017/S1759078722000113>

Chatterjee, A., Dey, P., Roy, K., & Parui, S. K. (2024). A Monolayer Frequency-Selective Surface for Wideband Shielding Application with Adequate Out-of-Band Separation and Angular Stability. *International Journal of Antennas and Propagation*, 2024(1). <https://doi.org/10.1155/2024/6692659>

Dey, S., & Dey, S. (2023). Broadband high gain cavity resonator antenna using planar electromagnetic bandgap (EBG) superstrate. *International Journal of Microwave and Wireless Technologies*, 15(1), 90–101. <https://doi.org/10.1017/S1759078721001768>

Gong, W., & Zhang, W. (2021). Design of Energy Selective Surface with Ultra-wide Protection Band. *Proceedings of the 2021 Cross Strait Radio Science and Wireless Technology Conference, CSRSWTC 2021*, 106–108. <https://doi.org/10.1109/CSRSWTC52801.2021.9631608>

Hu, N., Zhu, X., Wang, H., Yin, H., & Xu, Y. (2024). Design and analysis of response threshold of energy selective surface based on serial LC circuits. *International Journal of Microwave and Wireless Technologies*, 16(7), 1181–1186. <https://doi.org/10.1017/S1759078724000771>

Huang, R., Liu, J., & Liu, C. (2022). A Design of Pluggable High Power Microwave Protection Device in Waveguide. *2022 IEEE 9th International Symposium on Microwave, Antenna, Propagation and EMC Technologies for Wireless Communications (MAPE)*, 292–295. <https://doi.org/10.1109/MAPE53743.2022.9935211>

K. Sumathi, Lavadiya, S., Yin, P. Z., Parmar, J., & Patel, S. K. (2021). High gain multiband and frequency reconfigurable metasurface superstrate microstrip patch antenna for C/X/Ku-band wireless network applications. *Wireless Networks*, 27(3), 2131–2146. <https://doi.org/10.1007/s11276-021-02567-5>

K, A. S. B., & Pradeep, A. (2022). Complementary Metamaterial Superstrate for Wide Band High Gain Antenna. *2022 IEEE Wireless Antenna and Microwave Symposium (WAMS)*, 1–5. <https://doi.org/10.1109/WAMS54719.2022.9847735>

Kangeyan, R., & Karthikeyan, M. (2024). Circularly polarized implantable MIMO antenna for skin, brain and heart implantation with wide axial ratio bandwidth. *International Journal of Communication Systems*, 37(10). <https://doi.org/10.1002/dac.5778>

Luo, Z., Shan, X., Ren, X., Wu, K., Chen, Y., Hong, L., Ma, H. F., Cheng, Q., & Cui, T. J. (2023). Active Metasurface Absorber for Intensity-Dependent Surface-Wave Shielding. *IEEE Transactions on Antennas and Propagation*, 71(7), 5795–5804. <https://doi.org/10.1109/TAP.2023.3269160>

Melouki, N., Hocini, A., Fegriche, F. Z., PourMohammadi, P., Naseri, H., Iqbal, A., & Denidni, T. A. (2022). High-Gain Wideband Circularly Polarised Fabry-Perot Resonator Array Antenna Using a Single-Layered Pixelated PRS for Millimetre-Wave Applications. *Micromachines* 2022, Vol. 13, Page 1658, 13(10), 1658. <https://doi.org/10.3390/MI13101658>

Nguyen, D., & Seo, C. (2023). An Ultra-Miniaturized Circular Polarized Implantable Antenna With Gain Enhancement by Using DGS and Holey Superstrate for Biomedical Applications. *IEEE Access*, 11, 16466–16473. <https://doi.org/10.1109/ACCESS.2022.3174078>

Pannetier-Lecoeur, M., Fermon, C., Biziere, N., Scola, J., & Walliang, A. L. (2007). RF Response of Superconducting-GMR Mixed Sensors, Application to NQR. *IEEE Transactions on Applied Superconductivity*, 17(2), 598–601. <https://doi.org/10.1109/TASC.2007.898056>

Qin, D., & Zhang, W. (2019). Design of Energy Selective Surfaces with Wide Reflection Band. *2019 Computing, Communications and IoT Applications (ComComAp)*, 425–427. <https://doi.org/10.1109/ComComAp46287.2019.9018811>

Wang, K., Liu, P., Liu, H., & Meng, J. (2017). A miniaturized, self-actuated, energy selective spatial filter. *2017 IEEE 17th International Conference on Communication Technology (ICCT)*, 1689–1692. <https://doi.org/10.1109/ICCT.2017.8359918>

Wang, L., Tang, Z., Bao, H., & Ding, D. (2022). An Electromagnetic-Plasma Fluid Model Simulation of Waveguide Plasma Limiter Filled With Different Easily Ionized Inert Gas. *IEEE Transactions on Plasma Science*, 50(10), 3839–3847. <https://doi.org/10.1109/TPS.2022.3205968>

Yang, C., Liu, P. G., & Huang, X. J. (2013). A novel method of energy selective surface for adaptive HPM/EMP protection. *IEEE Antennas and Wireless Propagation Letters*, 12, 112–115. <https://doi.org/10.1109/LAWP.2013.2243105>

Zhang, J., Lin, M., Wu, Z., Ding, L., Bian, L., & Liu, P. (2019). Energy Selective Surface with Power-Dependent Transmission Coefficient for High-Power Microwave Protection in Waveguide. *IEEE Transactions on Antennas and Propagation*, 67(4), 2494–2502. <https://doi.org/10.1109/TAP.2019.2894274>

Zhou, L., Liu, L., & Shen, Z. (2021). High-Performance Energy Selective Surface Based on the Double-Resonance Concept. *IEEE Transactions on Antennas and Propagation*, 69(10), 7100–7107. <https://doi.org/10.1109/TAP.2021.3074770>

and Propagation, 69(11), 7658–7666.
<https://doi.org/10.1109/TAP.2021.3075548>

Zurauskiene, N., Balevicius, S., Zurauskaite, L., Kersulis, S., Stankevic, V., & Tolvaišiene, S. (2013). Nanostructured Manganite Films as Protectors Against Fast Electromagnetic Pulses. *IEEE Transactions on Plasma Science*, 41(10), 2890–2895.
<https://doi.org/10.1109/TPS.2013.2269480>

